

CENTRAL INTELLIGENCE AGENCY

INFORMATION REPORT

This Document contains information affecting the National Defense of the United States, within the meaning of Title 18, Sections 793 and 794, of the U.S. Code, as amended. Its transmission or revelation of its contents to or receipt by an unauthorized person is prohibited by law. The reproduction of this form is prohibited.

SECRET
SECURITY INFORMATION

COUNTRY	USSR (Kuybyshev Oblast)	REPORT	<input type="text"/>	25X1
SUBJECT	Activities at Zavod No. 2, Kuybyshev	DATE DISTR.	11 May 1953	
DATE OF INFO.	<input type="text"/>	NO. OF PAGES	38	
PLACE ACQUIRED	<input type="text"/>	REFERENCE NO.	RD	25X1
		REFERENCES		

This is UNEVALUATED Information

THE SOURCE EVALUATIONS IN THIS REPORT ARE DEFINITIVE.
THE APPRAISAL OF CONTENT IS TENTATIVE.
(FOR KEY SEE REVERSE)

25X1

25 YEAR RE-REVIEW

SECRET

STATE	#x	ARMY	#x	NAVY	#x	AIR	#x	FBI		AEC							
-------	----	------	----	------	----	-----	----	-----	--	-----	--	--	--	--	--	--	--

(Note: Washington Distribution Indicated By "X"; Field Distribution By "#".)

USAF review completed.

25X1

29

25X1

Page Denied

Next 5 Page(s) In Document Denied

SECRET

25X1

- 5 -

C. JUMO 022 TURBINE (For overall Sketch See Diagram #1)

25X1

1. Summarized Explanation to the Report about JUMO 022 Turbine.

The calculation and the design of the turbine had been charged to a group of engineers whose original working field had been exclusively the design of the Junkers propeller, and whose professional training was more in flow technique and wing theory than in thermodynamic turbine theory.

SECRET

SECRET

25X1

shortly before the scheduled 022 state test run. Eight to ten test power plants, previous to the state test run unit, had not achieved a satisfactory result in respect to either the full performance of the power plant and turbine or the specific fuel consumption.

25X1

The "Twisting" of the rotor blades of the third stage [redacted] resulted in a remarkable increase for the first time of the shaft performance, to $N_e = 5000 \text{ PS}_e$ with a specific fuel consumption $b_e \leq 300 \text{ g/PS}_e \text{ h}$. The pressure before the turbine increased only immaterially, which can be explained from the critical flows over large parts of the guide vane ring blade length (first and second stage).

25X1

With a new rotor blade setting of the third stage rotated -5° , the 022 power plant was released for the state test run.

Instead of now calculating and designing a blading without mistakes after a new method, test guide vane rings with blades turning on pins were ordered for all stages. At the same time a test arrangement of the 14-stage compressor with adjustable guide blades was ordered. That the power plant was improved by the experimental twisting of all compressor and turbine guide blades [redacted]

25X1

The experiments with exchangeable guide vane rings I, II, and III with $\alpha = 22^\circ$ and 25° were a failure.)

25X1

25X1

2. The 022 Power Plant Turbine Blading:

As ordered, the layout for power plant and turbine was to be for:

a propeller performance	$N_e = 5000 \text{ PS}_e$
airflow	$G^* = 30.0 \text{ kg/sec}$
compressor ratio	$\epsilon = \frac{P_1}{P_2} \cdot \frac{1}{6}$
specific fuel consumption	$b \leq 300 \text{ g/PS}_e \text{ h}$
for: ground conditions (operation on the test stand)	

SECRET

SECRET

- 10 -

25X1

No considerable participation of the thrust in the effective performance, complete removal of pressure in the turbine (eventually to subpressure for increase of the turbine flow diffuser-intermittent propulsive duct) (outlet velocity = flying velocity).

Discussed and used as basis for the design were:

Adiabatic compressor efficiency degree	$\eta_{adL} = 0.85$
Combustion chamber - combustion efficiency degree	$\eta_B = 0.96$
Combustion chamber - pressure decline	$\Delta P_B = 4\%$ of the compressor-pressure head.

Attempted at first was an adiabatic turbine efficiency degree of

$$\eta_{Tad} = 0.85.$$

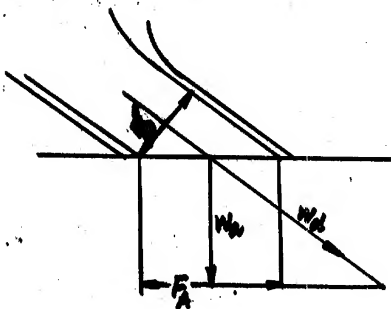
Based on previous research of constructed combustion chambers an intake velocity of the gasses of combustion to the turbine was arranged with

$$C_4 = 105 + 110 \text{ m/sec}$$

With the above data, only starting- and end-points of the expansion for the energy conversion in the turbine were fixed.

(an adiabatic rate of $H_{ad} = 110 \text{ cal/kg}$ corresponded to the nominal power at the above-mentioned data.) As auxiliary aid for the turbine design only a very inaccurate h-s existed at first. Later an especially calculated improved h-s diagram was available with specific heats C_p and C_v after Justi, and $R = 29.36$ for $\gamma = 4$.

In the turbine calculation and design a provisional lofting (contour) of the turbine was first designed, based on the above-described inlet and outlet conditions, with $\alpha = 0.5 + 0.6$. The number of blades was selected with consideration for sufficient blade overlapping. (Arrangement of the exit-nozzle duct with its influence on jet course and mutual periodical oscillation). In selection of the blade thickness in the exit plane the process in blade fabrication was taken into consideration. Therefore, the free axial channel flow cross-sections were fixed along the mean channel tube parallel to the turbine axis (later even under consideration of the heat expansion). Of the relations



$$F_D \cdot W_D = F_A \cdot W_A$$

$$\frac{F_A}{F_D} = \frac{W_A}{W_D} \cdot \sin \alpha$$

$$\frac{C_A}{W_A \cdot F_A} = \frac{C_D}{W_D \cdot F_D} = \gamma$$

ample use was made in fixing the blade angles.

This above adiabatic incline was now drafted into the h-s diagram, under utilization of the total-energy points T_{IV} , P_{IV} , V_{IV} and P_x , T_x , V_x and with the efficiency degree

$$\eta_T = \frac{P_{ad}}{P_{ad}} = 0.85$$

(See Diagram #2).

SECRET

25X1

SECRET

- 11 -

The flow velocities C_{10} to and from the turbine are calculated and superimposed on the corresponding adiabatics. That is:

$$\frac{C_4}{\sqrt{2}} = \frac{G^+}{F_{A4}} \quad \text{and} \quad \frac{C_{10}}{V_{10}} = \frac{G^+}{F_{A10}}$$

$$T_4 = T_{IV} - \frac{C_4^2}{2g} \frac{A}{C_{pm}/T_{IV}} \quad T_{10} = T_x - \frac{C_{10}^2}{2g} \frac{A}{C_{pm}/T_{10}}$$

$$\frac{p_{IV}}{p_4} = \left[\frac{T_{IV}}{T_4} \right]^{\frac{K}{K-1}} \quad \frac{p_x}{p_{10}} = \left[\frac{T_x}{T_{10}} \right]^{\frac{K}{K-1}}$$

These are the static (true) conditions in the beginning and end of the expansion.

3. Description of the Graphical Calculation Method with the H-s-Diagram for the Design of the O22 Turbines #1-10:

(See Diagram #3.)

25X1

25X1

The points P_4, T_4, v_4 , at the beginning of the turbine expansion, and P_{10}, T_{10}, v_{10} , at the end of the turbine expansion, were connected by the expansion polytrope. This static total drop was arbitrarily divided into three equal stage drops and the latter again, according to a reaction degree H_{st} rotor wheel/ H_{st} stator wheel = 1, divided into two equal part drops for rotor wheel and stator wheel.

It was tacitly assumed that the $\psi = \sqrt{\eta}$ values, as being dependent generally on the deflection angle and in case of the rotor blades--in a known way, as by Stadler--in addition on the head slot round flow (also the second and third guide vane ring permit a flow around the inner guide ring), could be achieved in conformity with the presumed turbine efficiency degree (and were also preserved). (Verbatim translation, unable to decipher.)

In determining the blade-exit angles the following system was used for all vane rings: (See Diagram #3.)

$$\frac{G^+}{F_{Ax}} = \frac{W_{Ax}}{V_{Ax}} = W_{Ax} \cdot \gamma_{Ax}$$

assuming:

$$\gamma = \frac{G^+}{F_A} \cdot \frac{1}{W_{Ax}} \quad \begin{matrix} W_{Ax} & = & 100 & 200 & 300 & \text{ms}^{-1} \\ & & X & Y & Z & \text{kg m}^{-3} \end{matrix}$$

$$\begin{matrix} \text{Polytropic expansion } \gamma_{123} = U & V & W & \text{m}^3 \text{ kg}^{-1} \\ \text{assumed on the true} & & & \\ \text{(static) polytropic} & & & \\ \text{state:} & \gamma_{4123} = \frac{1}{U} & \frac{1}{V} & \frac{1}{W} & \text{kg m}^{-3} \end{matrix}$$

appertaining speed $H = r \quad s \quad t \quad \text{cal / kg}$
from the diagram:

$$W_{Ax} = \sqrt{8360 \cdot H} \cdot \sin \sigma \quad (\text{This angle has to be determined.})$$

But now the performance share for each stage corresponding to the expansion has to be transmitted on the rotor wheel. (See Diagram #4.) The directions of the absolute exit velocities from the rotor wheels were assumed to be parallel to the axis. Therefore, a further conditional equation was:

SECRET

SECRET

- 12 -

25X1

$$\frac{1}{g} V_1 W_1 \cos \sigma_1 = \frac{n}{n-1} (P_1 V_1 - P_2 V_2) = \frac{n}{n-1} R T_1 \left[1 - \left(\frac{P_2}{P_1} \right)^{\frac{n-1}{n}} \right]$$

$$W_1 \cos \sigma_1 = \frac{g \frac{n}{n-1} (P_1 V_1 - P_2 V_2)}{V_1} = \frac{g \frac{n}{n-1} R T_1 \left[1 - \left(\frac{P_2}{P_1} \right)^{\frac{n-1}{n}} \right]}{V_1}$$

In this way it would have been possible (as sketched in Diagram #3) to interpolate on the pertinent $\frac{W_D \sin \sigma}{V} = \frac{G}{FA} \sin \sigma$ in a procedure

similar to the x^2 -method with various assumed W_D , to the polytrope transmitted $W_D^2 \frac{A}{2g}$ and from the polytrope read off $V = \frac{1}{\phi}$.

25X1

During the layout calculations every blade length was subdivided four times along the blade length for determining the necessary twists for the condition: $\frac{U \cdot C}{A} = \text{Constant}$

This and the following circumstance made the calculations nearly uncontrollable.

The first test-power plants were far below the rated performance of $N = 5000\text{PS}$, with very high specific fuel consumption. For this reason a new blading design was laid out for better turbine efficiency degrees. It was based on the very courageous assumption that the course of the preselected polytrope (very steep and nearly falling in line with the adiabatic) would have to follow the static change of condition, if the blade angles and nozzle cross sections had been rated correspondingly.

by this method the turbines could perform worse rather than better.

25X1

The definition of the flow loss factor $\phi = \sqrt{\eta}$ and the definition of the nozzle efficiency degree η

$$\phi_{co} = \sqrt{\eta_{co}} = \sqrt{\frac{H + C_4^2 \frac{A}{4}}{H^2 + C_4^2 \frac{A}{4}}}$$

According to this relation ϕ and η both increase with increasing flow velocity-- until the limiting value of critical flow and approach a limiting value $\phi = \sqrt{\eta} = 1$. (But an impulse or constant pressure turbine with $\eta \rightarrow 1$ does not exist.)

25X1

It is a well-known fact that lesser losses appear by curvature flow, if the gas expands at the same time in the flow channel and avoids detachment of the flow from the channel wall (from the curved wing).

The above-mentioned definition of the efficiency degree contradicts this simple fact in the beginning.

The sketched h-s diagrams (in Diagram #4) which generally can be applied to all six turbine blade nozzle channels, are designed for critical flow at the temperature T_5 with

$$W_{kv} \approx \sqrt{g \times R T_5}$$

SECRET

Page 11 of 21

SECRET

25X1

- 13 -

with friction more accurately $w_{kv} = \sqrt{g \frac{x}{x-1} (n-1) R T_5}$

for each of the three h-s diagrams equal, equal "n" from $\eta \frac{x-1}{x+1} = \frac{n-1}{n+1}$

also equal "n" supposed (equal $x = f(T)$, of course.)

Then also $\frac{p_{IV}^1}{p_5^1} = \frac{p_{IV}^{11}}{p_5^{11}} = \frac{p_{IV}^{111}}{p_5^{111}} = \left(\frac{2}{n+1}\right)^{\frac{n}{n-1}}$ are equal critical

pressure ratios.

But $\frac{p_v}{p_5}$ is not a critical pressure ratio.

Since the gas flows critically also in point $T_5; p_5; v_5$

Then $\frac{p_{IV}}{p_5} = \left(\frac{2}{m+1}\right)^{\frac{m}{m-1}}$ should become a critical pressure ratio.

This can be achieved through introduction of a new definition for the efficiency degree $\eta_{co} = \frac{H + C \frac{1}{2} \frac{v^2}{g}}{H + C \frac{1}{2} \frac{v^2}{g}} = \frac{2\epsilon + 1}{2\epsilon - 1} \cdot \frac{m-1}{m+1}$

and through introduction of a new polytropical exponent "m".

But one cannot imagine one and the same process of polytropic expansion at the same time with two different polytropic exponents and efficiency degrees: First with

$1/\eta = g^2 = \int (\text{channel for } \eta^2) \text{ and secondly: with an arbitrarily created } \eta_{co} \text{ and } m.$

This analysis of the critical flow behavior and the analysis of the efficiency degrees at the curvation flow point to the mistakes which have been made, but still do not touch the main reason.

The essential point is a misunderstanding and the wrong use of the h-s diagram in general, when with it static changes of conditions of a gas are handled. The heat content of static gases is u and not h. The process of treatment of condition changes of static gases in an h-s diagram is a mistake; they can only be followed by means of a p-v, or also a T-s diagram. The h-s diagram is made for adiabatic expansion (and compression) for entering and leaving flowing gas. (Each polytropic expansion between two intentional pressures of a gas results in greater work as the adiabatic.) The total energy content in flowing gas consists of the sub-amounts.

$$h = v + p.v + c^2 \frac{A}{2g}$$

These amounts cannot be kept separated in the h-s diagram.

25X1

With a practical η_p , which gives evidence that only a part $c^2 \frac{A}{2g}$ of the total energy drop $\Delta h_{\text{Total}} = \Delta U + \Delta p.v + c^2 \frac{A}{2g}$ can be gained

SECRET

SECRET

25X1

- 14 -

in the expansion in the turbine blade channel (the data for $\varphi = \sqrt{\eta}$ depending on the deviation angle, the channel form and the tip slot flow, are widely spread in technical literature)

25X1

the blade channel nozzle cross sections and therewith the blade angles were determined.



4. The Turbine Bearing:

The turbine bearing reached very high temperatures during operation, whereby its rotating qualities and lifetime performance were unfavorably influenced. Furthermore, considerable quantities of lubricating oil infiltrated from the storeroom ($p_2 \approx p$ outside) into the cooling air storage ($p_k \approx p_4$). Since several bearings failed during test operations, and all bearings showed bad cartographics, changes had to be made. A new development for the bearing had to be found. (See Diagram #6, Sketches 1 and 2.)

25X1

In the case of the turbine bearing constructional errors and deficiencies produced the unsatisfactory bearing performance:

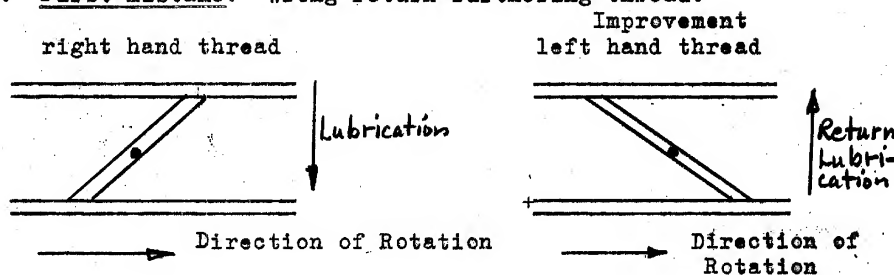
SECRET

SECRET

25X1

- 15 -

- a. First mistake: Wrong return-furthering thread!



- b. Second mistake: Every rapidly turning bearing has a strong pumping effect.

25X1

_____ This area was open toward the outside only by a slot, through which oil should not flow. Furthermore, no flow channel for the intended cooling air stream existed (except the above-mentioned sealing slot).

- c. Third mistake: The solidity of the shaft was very doubtful because the omission of the fillet in the transition from the shaft to the flange.

- d. Fourth mistake: According to the above, the lubrication as intended by the chiefs was very questionable in respect to improvement of the cooling, and therewith improvement of the operational quality and packing.

25X1

Sketch 1 (of Diagram #7) is significant because of large channels for relief of the area back of the rollers and for passage of the cooling air (from inside and from outside). This bearing was installed in the turbines for the state test run.

Sketch 2 (of Diagram #7) is a further improved design _____. It provided a splash ring constructed as a rotor for amply supplying cooling air and therewith safe lubrication supply for the bearing. Also the splash ring would insure that the lubricating oil, which was blown off the rollers, was directed into the slot. The mounting of the whole roller bearing in a closed casing should exclude damaging the bearing at the assembly of the shaft. _____ another drawing (Diagram #8) _____ is an additional sketch of the bearings and their relation with the turbine assembly.

25X1

25X1

25X1

D. THE THRUST NOZZLE

According to orders, the relative share of thrust on the effective total performance of the O22 power plant should be as small as possible. That meant the exit velocity c_{11} of the gas from the thrust nozzle should be as low as possible. The turbine gases should be reduced to the energy level of the outside pressure of a motionless power plant on the test stand. Under consideration of flight condition, $c_{11} = 200 \text{ m/s}$ was selected.

Only a short diffuser for the thrust nozzle could be contemplated because of the prescribed measurements of the inlet cross section of the thrust nozzle.

SECRET

SECRET

- 15 -

25X1

However, the construction office delivered a contracted nozzle which was even more converging than planned. It had not been taken into consideration that the smallest flow cross section is still considerably smaller than the axial free cross section. For this reason this thrust nozzle was officially changed (as shown in Sketch 1 of Diagram #9).

After a short time in operation the inner covering broke at the holes for the support arms (Sketch 1).

Despite removal of the throttle points in the thrust nozzle, the brake horsepower from the turbine remained far below the rated values in the beginning.

$$N_{ET} = N_{EL} + N_{EW} = G^+ \eta \cdot \frac{2g}{x-1} RT_{IV} \left[1 - \left(\frac{p}{p_{IV}} \right)^{\frac{x-1}{x}} \right]$$

Pressure: $p_{IV} = 4.5 \quad 4.8 \quad 5 \quad 5.3 \quad 5.5 \quad 6 \text{ kg cm}^{-2}$
 $N_{ET} = N_{EL} = N_{ED} = 3200 \longrightarrow 5000 \text{ PS}$

To achieve the highest possible performance on the shaft, the temperature T_{IV} was raised but this also made the exit temperature and the thrust undersirably high.

As a countermeasure all later test runs for approximately two years were performed without thrust nozzles. The gas escaped from the back of the turbine.

Dr Cordes thought that a hood screwed to the last turbine wheel and rotating with it could not be realized as a substitute for a nozzle. Such a rotating body in the desired proportions could not be built solidly enough ($\frac{1}{2} \rho v^2 \geq 25 \text{ kg mm}^{-2}$).

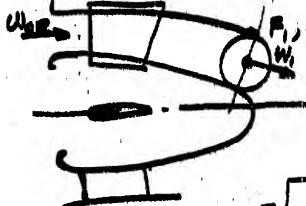
Shortly before the O22 state test run deadline the thrust nozzle (rather the diffuser) was designed (according to Sketch 2 in Diagram 9). Here a version of the O12 thrust nozzle was adopted because the originally selected O22 construction proved not to be breakproof.

25X1

25X1

(here at the positive diffuser)

P_0, P_0, T_0 $\eta = \frac{2g(1-f)}{1-2g} > \eta$ in the relations:



$$W_{or} = \sqrt{2g \frac{x}{x-1} P_0 V_0 \left[\left(\frac{P_1}{P_0} \right)^{\frac{x-1}{x}} - 1 \right] + W_1^2} \cdot M^{-1}$$

$$\frac{V_1}{V_0} = \left(\frac{P_0}{P_1} \right)^{\frac{1}{x}} \quad V_0 = \frac{P_0 V_0 A}{G^+} = \pi^3 \text{ kg}^{-1}$$

$$F_1 = \frac{G^+ V_1}{W_1}$$

SECRET

SECRET

- 16 -

25X1

E. ANNULAR COMBUSTION CHAMBER

The various parts of the combustion chamber of the Jumo 022 (as shown in Diagram #10) are as follows:

Part #1: 12 pieces, combustion chamber head: parabolic hollow object, passing into a circular ring sector. Approximately three mm slot between the single sectors. The 12 heads were welded to a closed ring.

Part #2: 12 pieces; preheating chamber for combustion air; welded within combustion chamber head.

Part #3: 12 pieces; turbulence rose, welded within Part #2. A slide fit was provided for the fuel nozzles.

Part #4: 12 pieces; stiffening metal with "heart shaped hole". Combustion chambers without this stiffening metal piece tested previously always ripped between the heads. With the stiffening metal pieces added, the flow through the air slots was impaired. Addition of the heart-shaped holes permitted air masses to flow into the combustion chambers.

Part #5: 1 piece; cylindric outer envelope

Part #6: Approximately 140 pieces; outer secondary air mixers

Part #7: 1 piece; conic inner envelope

Part #8: Approximately 140 pieces; inner secondary air mixers

Material for part 5, 6, 7 and 8 were 3017 with a sheet metal thickness of 1 mm at first and later increased to 1.5 mm.

Part #9: 1 piece; outer stiffening ring

Part #10: 1 piece; inner stiffening ring

Part #11: 12 pieces; socket piece for glow plugs

25X1

All parts were carefully welded using the best equipment. The sheet metal thickness was raised from one mm to 1.5 mm by an annealing operation in aluminum powder (filings) by a diffusion process. In this way parts touched by flame could be largely protected. However, is the best heat resistance also raised by this procedure?

Nevertheless, dents and breaks which reduced the life of the chambers always appeared on the combustion chambers.

According to the opinion of the experts these repeating breaks were solely caused by the oscillations of the thin sheet metal body.

SECRET

SECRET

25X1

- 17 -

[redacted] deformation by bending moments conditioned by the general layout of the combustion chamber largely contributed to the dents and breaks of the metal. The hollow body, which was originally supported only in the planes X and Y (see Diagram #11) and cantilevered between the planes Y and Z, was very soft and subject to vibration. During the development, the turbulence rose was built in for combustion reasons. The bore of this turbulence rose with the pin of the fuel nozzle connection formed a third bearing in the plane "Z" and a "straightening" of the combustion chamber head in a concentric-conic axis.

25X1

If the hollow body were supported only in the planes X and Z, then the forced moments M_x were avoided, but the general bending moment becomes greater again and the danger of vibration breaks increases.

25X1

[redacted] A stator ring after the compressor rotor wheel #14 would be very desirable for two reasons. One was the consideration for a more even flow. The second was for support of the bearing cantilevered from the first turbine stator stage.

But all these considerations were above the "horizon" of the present specialists. The first designs and construction forms of the combustion chamber suffered due to the fact that the technical designers had previously worked on construction of formers or were auxiliary draftsmen nearly their whole lives.

The layout of the BMW-024 annular combustion chamber could have been a good guide.

Appendix to the chapter on combustion chamber:

[redacted] sketch (Diagram #11) shows the original construction form of the 022 annular combustion chamber consisting of:

25X1

Part #1: 1 piece; cylindric metal casing, thickness of - 1 mm, with outer secondary air mixers.

Part #2: 1 piece; inner conic metal casing, - 1 mm with inner secondary air mixers.

Part #3: 12 pieces; parabolic combustion chamber head, conically arranged and penetrating each other at "A" connected to #1 and #2 at "B" and "C" (coupled). The overlapping edge "A" was welded and gave a fairly good flow profile for the mixed air flowing

SECRET

SECRET

25X1

- 18 -

near the heads. The intake nozzles into the heads were simply bent. Staggered-arranged ram tubes "H" guided the combustion air into the combustion area "R". The whole hollow body was supported by "X" at the outlet of the chamber in the turbine stator first stage and by the screw of the glow plug at "Y". The bores "Z" were later installed for improvement of the combustion. This original construction was in no way satisfactory. The combustion efficiency was very bad. After a short test run only an unrecognizably dented and torn metal body was left.

But the contours given in this thoughtless unprofessional design were also later binding for the new construction to achieve better combustion and longer life. Better combustion was achieved through the addition of an expansion nozzle in the combustion chamber head (creation of a pre-heating chamber for the combustion air) and by superimposing of a turbulence throttle - both taken from an excellent description of single combustion chambers in British-American power plants with 99.7% combustion efficiency.

Because of the conically arranged nozzles - their pins should support the combustion chamber on the heads - the combustion chambers were still always dented and torn despite all sorts of stiffenings.

Following are the considerations

which in all probability do not check with the actual measures taken.

As a sample for an exemplary, solid construction in regard to the support of the combustion chamber, drawings and parts of the BMW-024 power plant were available. According to this model the 022 combustion chamber should have been laid out (shown in Diagram #12).

Part A: 6 pieces; supporting profile arms between every second combustion chamber head.

Part B: 1 piece; inner support cone, welded at "C" with "A".

Part D: 1 piece rotating nose ring, welded on support arms "A"; between the combustion chamber heads added to the (rotating) profile ring "E".

Part F: 6 pieces; combustion chamber heads "F", mounted into the profile ring "E". The rear end of the heads welded into two concentric circular strips "G" and "H".

On these circular strips ("G" or "H") are:

Part I: 1 piece; outer casing with outer secondary air mixers.

Part K: 1 piece; inner casing with inner secondary air mixers.

Part L: 12 pieces; intake nozzles, welded to the nose ring and shapes.

The sketch shows, for the sake of completeness, the injector assembly with the injection nozzles and the so-called disks for mixing in the BMW construction.

The whole construction is overloaded and heavy and cannot be recommended because the radially located side walls of the ring sectors' warped

SECRET

SECRET

- 19 -

ends of the parabolic combustion chamber heads are parallel to the support profiles "A".


The following construction form can be regarded as the best solution.

Fuel injection nozzles arranged with support pins parallel to the power plant axis. This demands a slightly changed construction of the turbine casing.

25X1

25X1

F. AXIAL COMPRESSOR

The following parts are identified in  sketch of the axial compressor (see Diagram 13):

25X1

Part 1a: 1 piece, compressor casing:

Divided in horizontal axis (parallel to axis) consisting of:

Part 1: 1 piece; outer casing metal, 1.5 mm thick

Part 2: 4 pieces; longitudinal flange

Part 3: 2 pieces; flange

Part 4: 13 pieces; -ring

Part 5: 13 pieces; stator ring

Part 2a: 13 pieces; stator ring, complete, consisting of:

Part 7: 1 piece; outer stator ring

Part 8: 1 piece; inner stator ring

Part 9: stator blades

} Steel welded gas welding

Part 3a: 1 piece; compressor rotor, complete, consisting of:

Part 10: 14 pieces; wheel disk, new construction form without hollow shaft and flange (see Diagram #1).

Part 11: various; light metal blades, with dovetail foot strip.
Material: alloy, hammered in die, afterward worked over and recently also finished in die (pressure die casting?).

Single wheel disk, statically balanced:

Part 12: 13 pieces; plug adapter (structural element of the hollow shaft with flanges), only in new construction form of rotor (see Diagram #1).

Part 14: 1 piece; front flange shaft

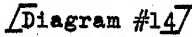
Part 15: 1 piece; rear flange shaft

Part 16: 1 piece; labyrinth split gasket ($G_L^+ = 1.5 \text{ kg/sec}$)

Complete compressor rotor statically and dynamically balanced

G. COUNTER-ROTATING PROPELLER MAIN GEARING

1. Constructed gears:

A sketch  shows essentially the construction of the propeller reduction gear, scaled M = 1:5 in full power flying operation with

SECRET

SECRET

25X1

- 20 -

$n_1 = + 6000 \text{ min}^{-1}$ and $N_1 = 5000 \text{ PS}_0$
 front prop $n_2 = + 1000 \text{ min}^{-1}$ and $N_2 = 2500 \text{ PS}_0$
 rear prop $n_3 = - 1000 \text{ min}^{-1}$ and $N_3 = 2500 \text{ PS}_0$

The drive-sun gear I is driven with n_1 from the front end of the compressor shaft over drive shaft 1. The planetary gear II, rotating with $N_1 = 5660 \text{ min}^{-1}$, drives

- a. the web 6 through its axis 5 and the shaft 2 with $n_1 = + 1000 \text{ min}^{-1}$, and
- b. the hollow shaft 3 by meshing with the inner toothed central gear #III.

Parts 7 and 8 on the secondary drive shafts carry the heavy controllable-pitch propeller hub bodies. The propeller control gears (geared oil motors with planetary gears) (see Diagram #15) are mounted within the hub.

A geared oil pump regulated by the speed governor supplies the Servomotors in the propeller control gears V through a piping system inside the hollow shafts. This way the number of revolutions of the counter-rotating propellers is regulated to $n_2 = + 1000$ and $n_3 = 1000 \text{ min}^{-1}$.

By the selection of the gear ratio, appropriate deviating numbers of revolutions are:

- a. front propeller: $n_2^I = + 1000$ and $n_2^{II} = 900 \text{ min}^{-1}$
 rear propeller: $n_3^I = 860$; $n_3^{II} = 1140 \text{ min}^{-1}$
- b. rear propeller: $n_3^X = 1100$; $n_3^{XX} = 900 \text{ min}^{-1}$
 front propeller: $n_2^X = 928$; $n_2^{XX} = 1072 \text{ min}^{-1}$

If the feathering is applied completely to the front propeller, $n_2 = 0$, the rear propeller with $n_1 = 6000 \text{ min}^{-1}$, would build up to $n_3 = 2400 \text{ min}^{-1}$. If the feathering is applied completely to the rear propeller $n_3 = 0$ then at $n_1 = 6000 \text{ min}^{-1}$, the front propeller would build to $n_2 = 1720 \text{ min}^{-1}$. This takes place providing the performance equilibrium between turbine and propeller performance permits the number of revolutions.

The fluctuations from a synchronized run which were frequently observed in test operations on the test stand were considered as a serious malfunction.

25X1

A turning moment $M_{dp} = 596 \text{ mkg}$ was transmitted to the power plant from the gear box which could be used to measure the performance.

The operation of the gearing was safe as far as solidity and life were concerned. Additional oil cooling provided by bores "O" was required at the central sun gear I, because of frictional heating.

2. Designs:

the design of a gear for the

25X1

SECRET

SECRET

- 21 -

012 propeller power plant. (The construction of such a gearing is 25X1 shown in Diagram #16.)

The transmissions

$$\varphi_1 = n_1/n_2 = \frac{+6000}{+1000} = +6:1 \quad \text{and}$$

$$\varphi_2 = n_1/n_3 = \frac{+6000}{-1000} = -6:1$$

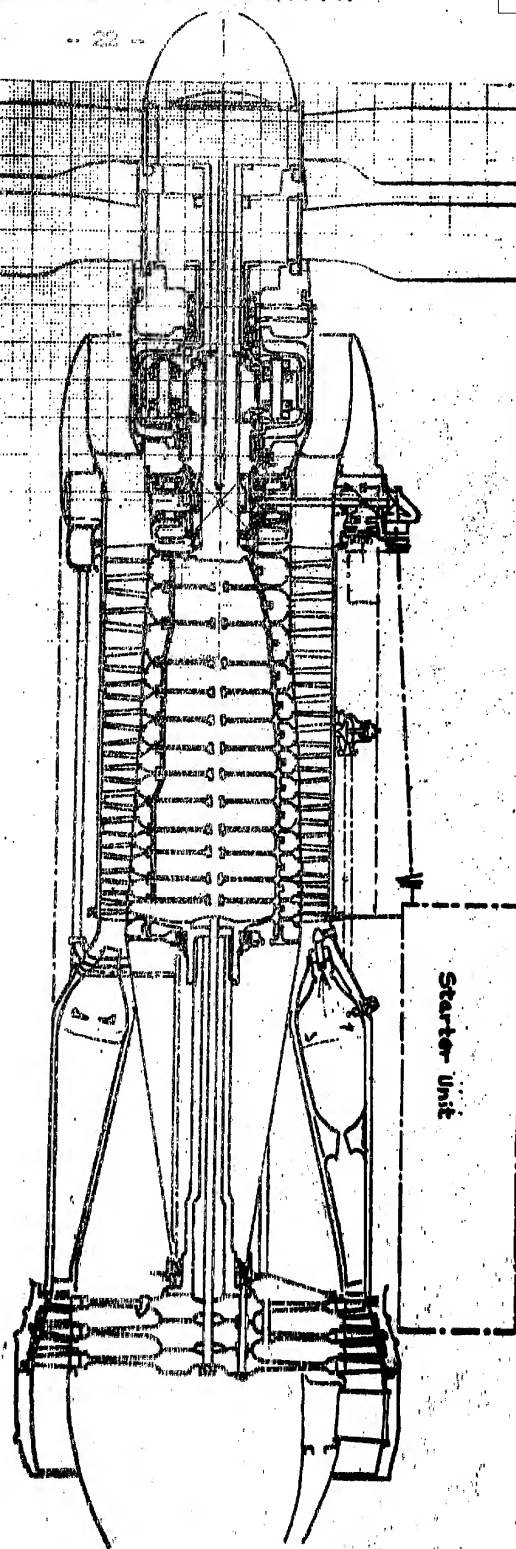
25X1

and the performance distribution are here compulsory. Everything else concerning such a gearing is mentioned in Diagram #16.

- DIAGRAM (1) Turboprop Power Plant
- DIAGRAM (2) H - S Diagrams
- DIAGRAM (3) Determination of Blade Exit Angles
- DIAGRAM (4) H - S Diagrams for 3 Turbine Stages
- DIAGRAM (5) Sheet #1 - Turbine Flow Channel
Sheet #2 - Turbine Flow Channel showing Blade Positions along the Mean Flow
- DIAGRAM (6) Turbine Bearing Installations as Designed by Turbine Department
- DIAGRAM (7) New Designs for Turbine Bearing Installations
- DIAGRAM (8) Turbine Arrangement (Bearings and their relation to Turbine Assy)
- DIAGRAM (9) Jumo 022 Thrust Nozzle
- DIAGRAM (10) Annular Combustion Chamber
- DIAGRAM (11) Combustion Chamber and Turbine Casing Development (First Form)
- DIAGRAM (12) Combustion Chamber and Turbine Casing Development (Not Constructed)
- DIAGRAM (13) Axial Compressor Design
- DIAGRAM (14) Counter Rotating Propeller Main Gear (Jumo 022)
- DIAGRAM (15) Propeller Control Gears
- DIAGRAM (16) Propeller Gearing for Jumo 012

SECRET

SECRET—SECURITY INFORMATION



TURBOPROP POWER PLANT

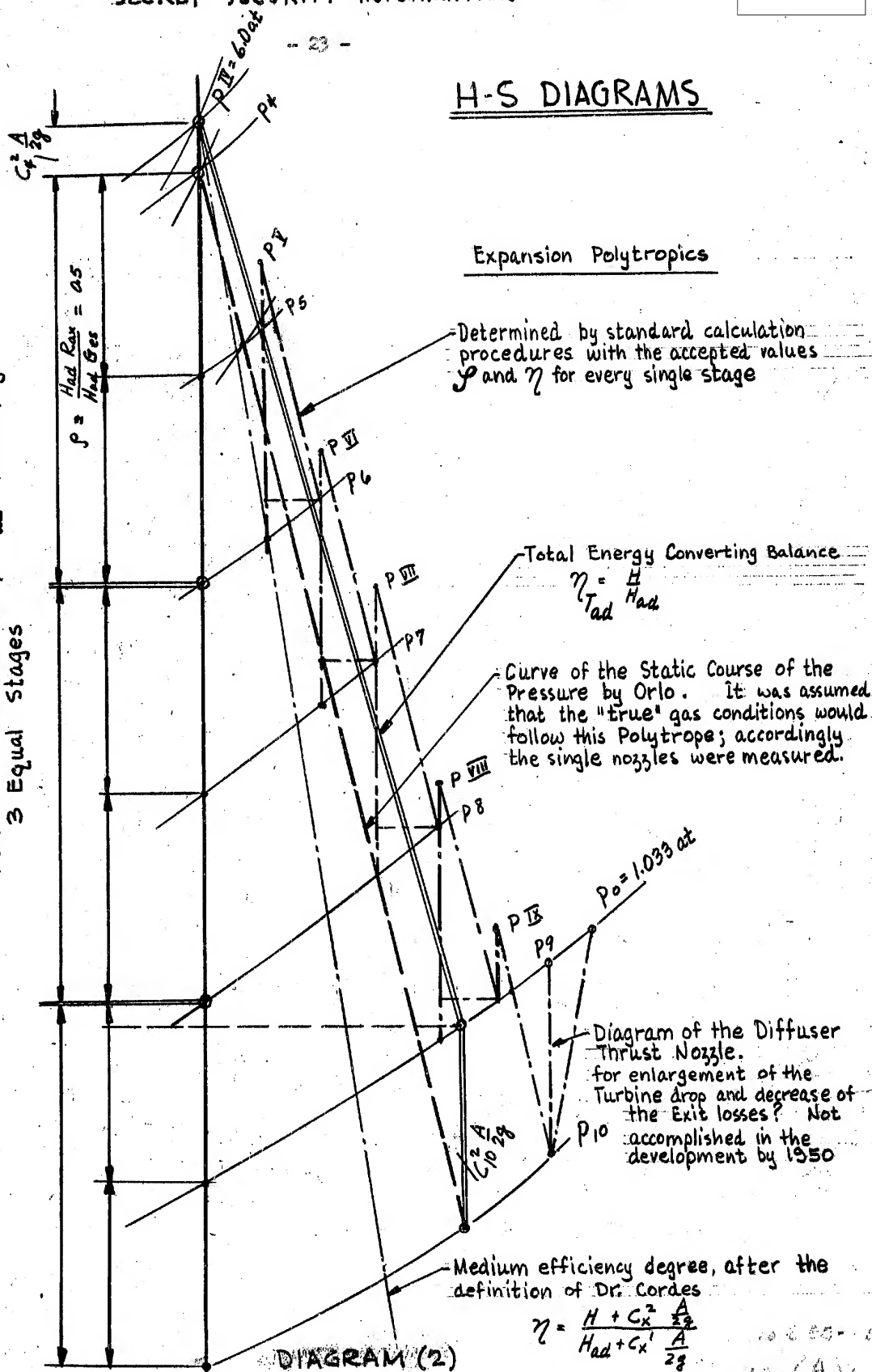
Ne-5000 P5c Propeller Performance

Scale : 1 = 15.62

**G = 340 m/sec, C = 5316.0
h = 8002/m.s**

DIAGRAM (1)

SECRET—SECURITY INFORMATION

SECRET-SECURITY INFORMATION**H-S DIAGRAMS****Expansion Polytropics**Adiabatic rate at Full Power, $H_{ad} = 110 \text{ cal/kg}$
3 Equal Stages**- SECRET -**

SECRET- SECURITY INFORMATION

- 24 -

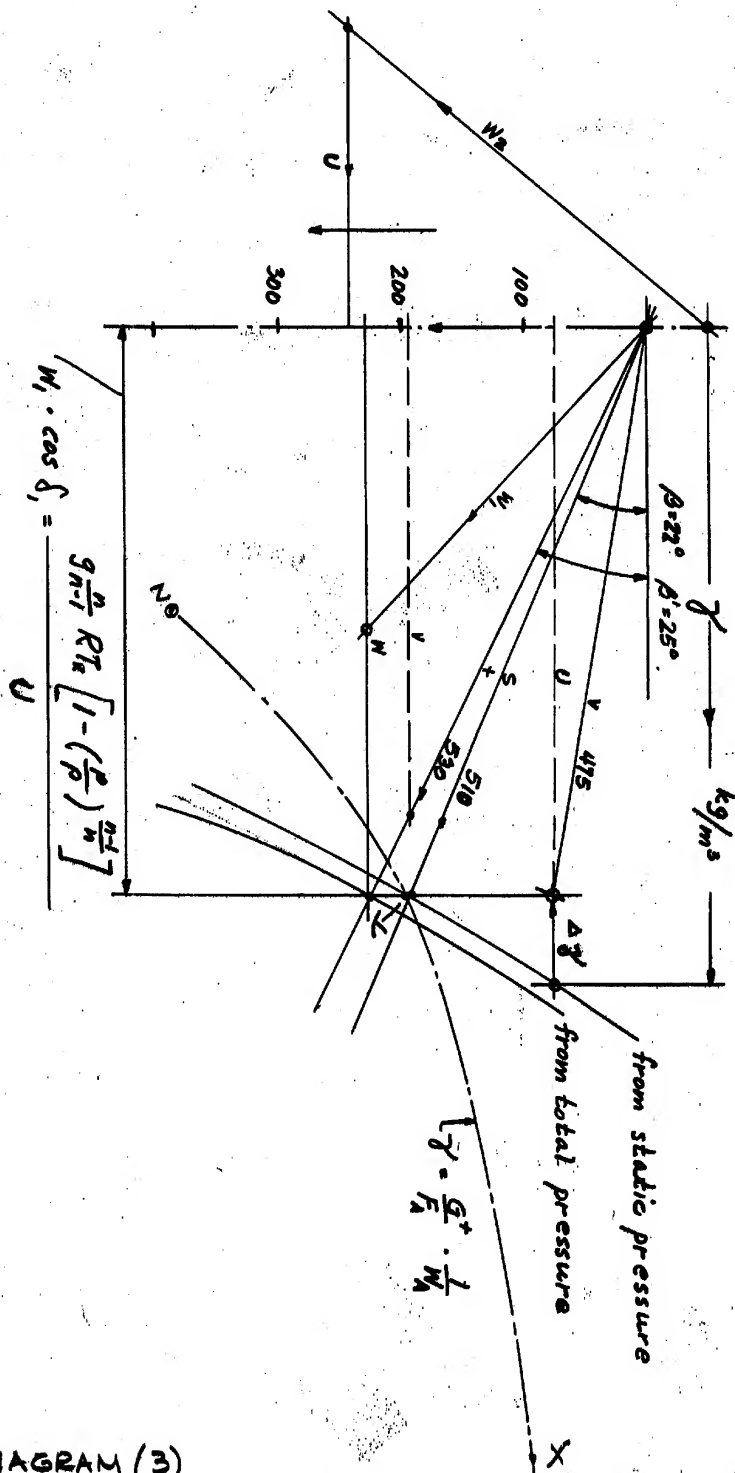
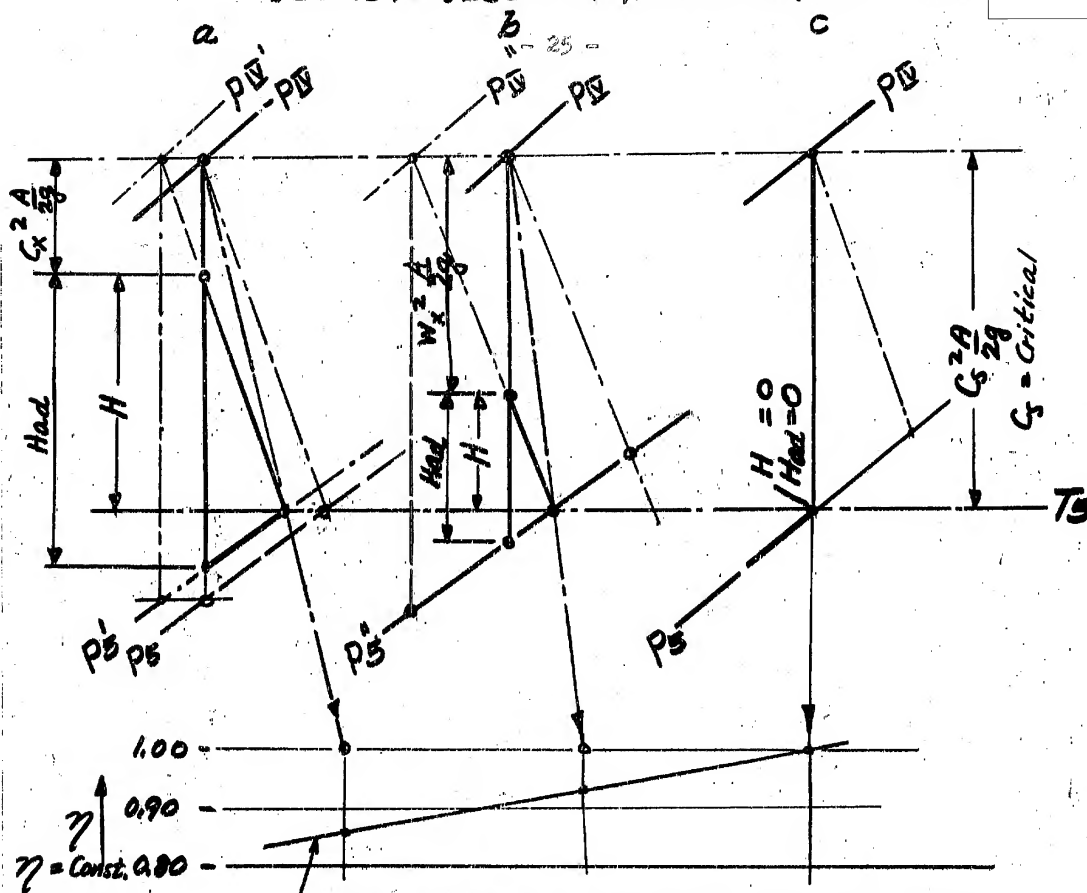


DIAGRAM (3)
DETERMINATION OF BLADE EXIT ANGLES

-SECRET-

SECRET- SECURITY INFORMATION



Course of the efficiency degree, after

a relation by Dr. Cordes
$$\eta_{ad} = \frac{H + C_x^2 \frac{A}{2g}}{H_{ad} + C_x^2 \frac{A}{2g}} = \varphi^2$$

NB
Wrong Conclusions
Nozzle with
Pre-Velocity

Used for more than three years in Blade design.

Reaction Wheel

Action Wheel



Section A-B



Flow produces
throttling and
loss

separation

H-S DIAGRAM for THREE TURBINE STAGES

DIAGRAM (4)

- SECRET -

SECRET-SECURITY INFORMATION

- 26 -

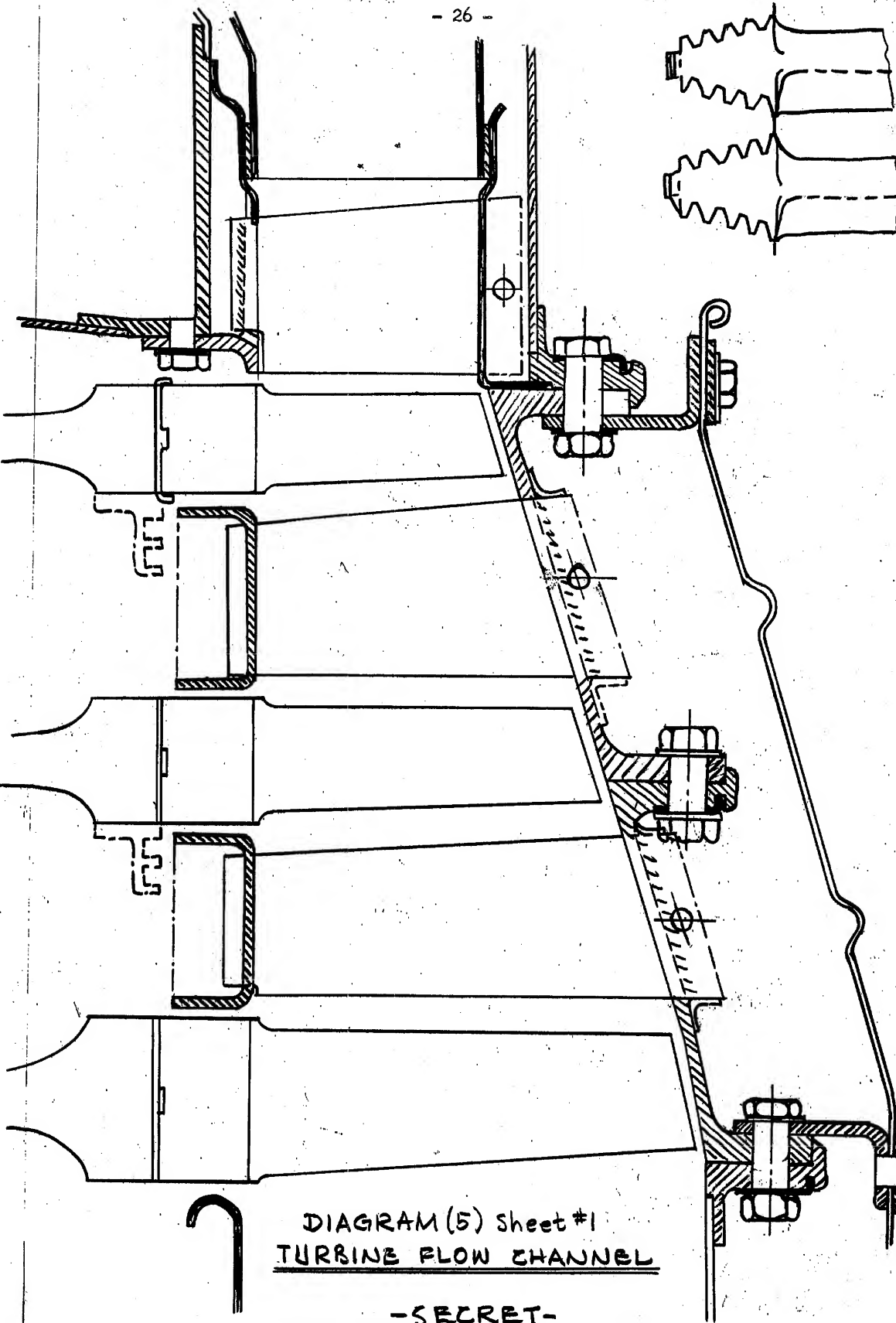
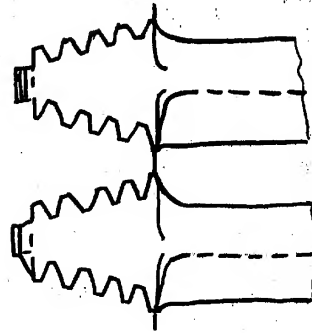
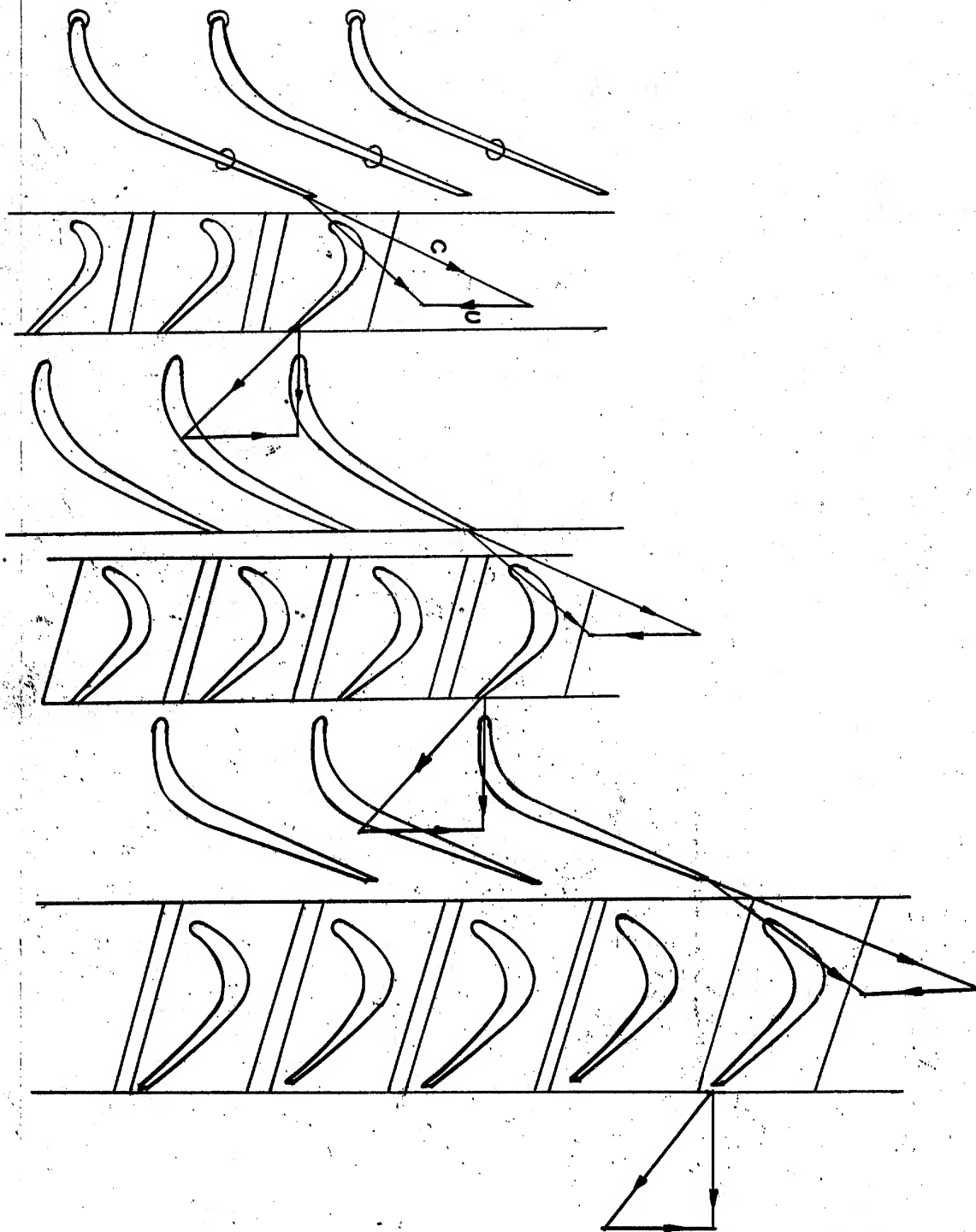


DIAGRAM (5) sheet #1
TURBINE FLOW CHANNEL

-SECRET-

SECRET - SECURITY INFORMATION

- 27 -



TURBINE FLOW CHANNEL SHOWING BLADE
POSITIONS ALONG THE MEAN FLOW
DIAGRAM (5) Sheet #2

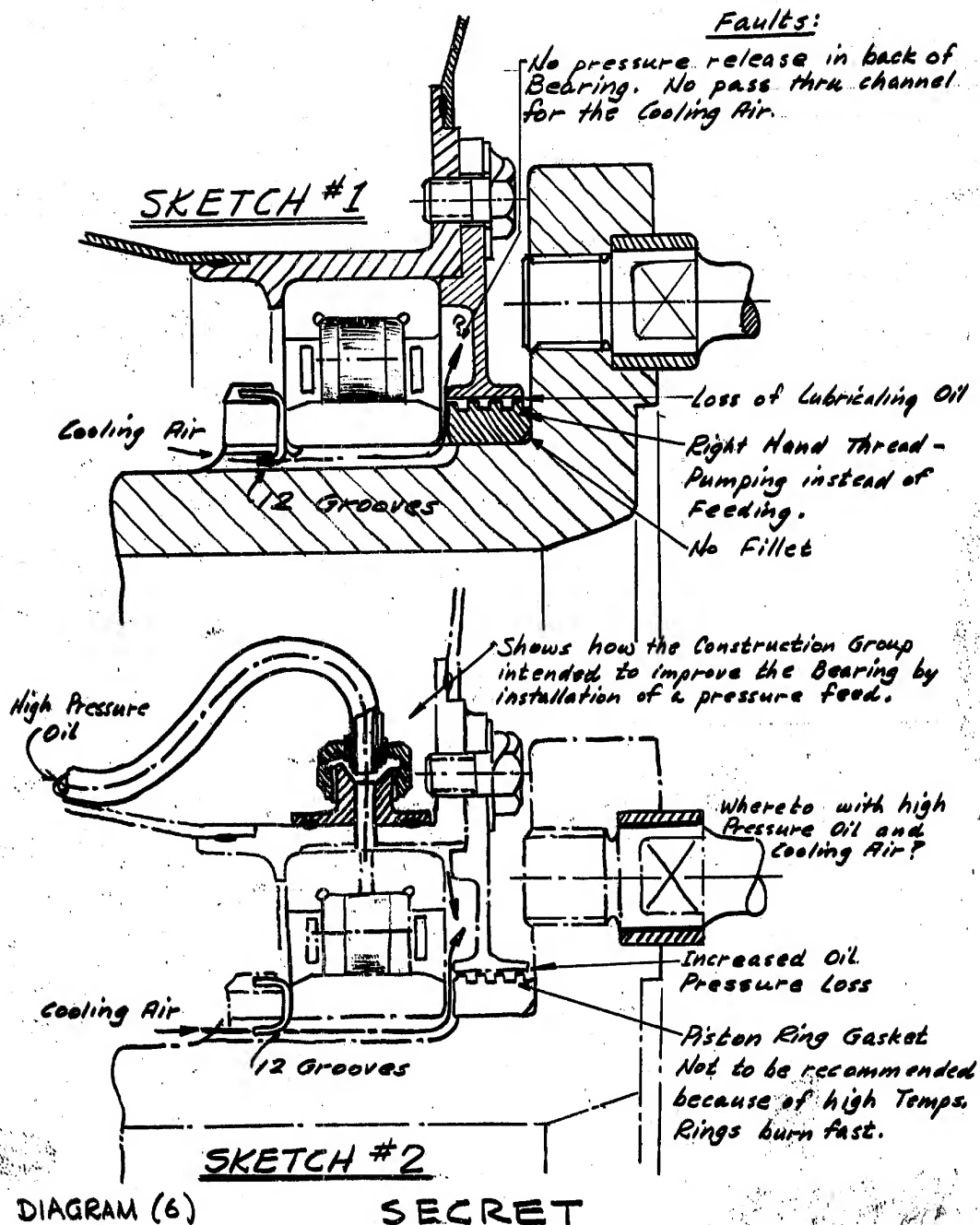
SECRET

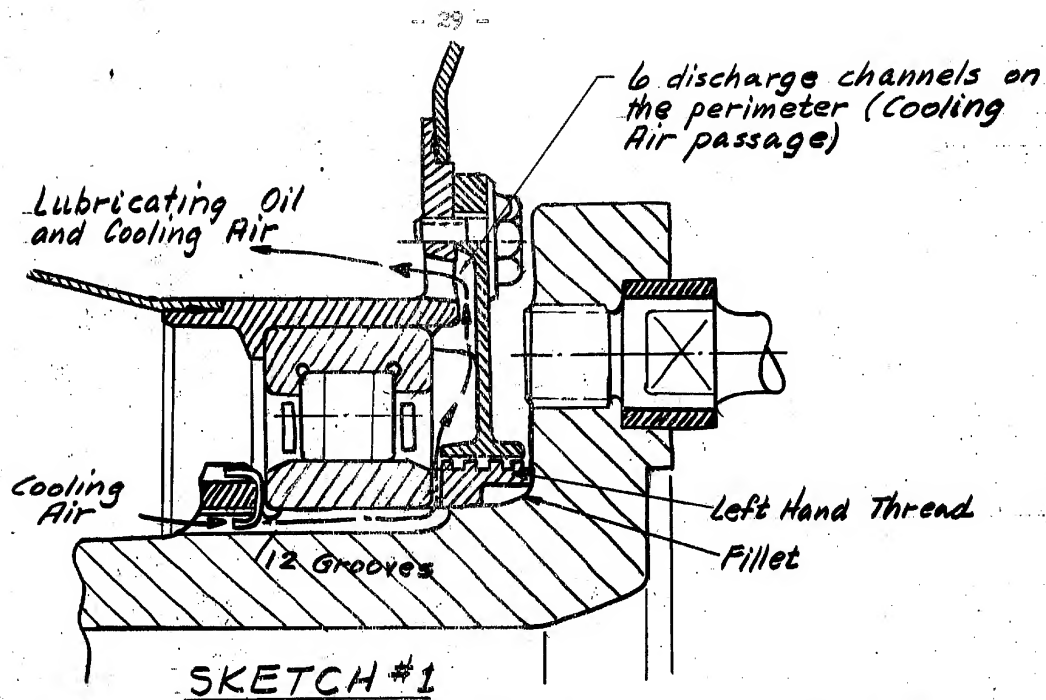
SECRET-SECURITY INFORMATION

- 28 -

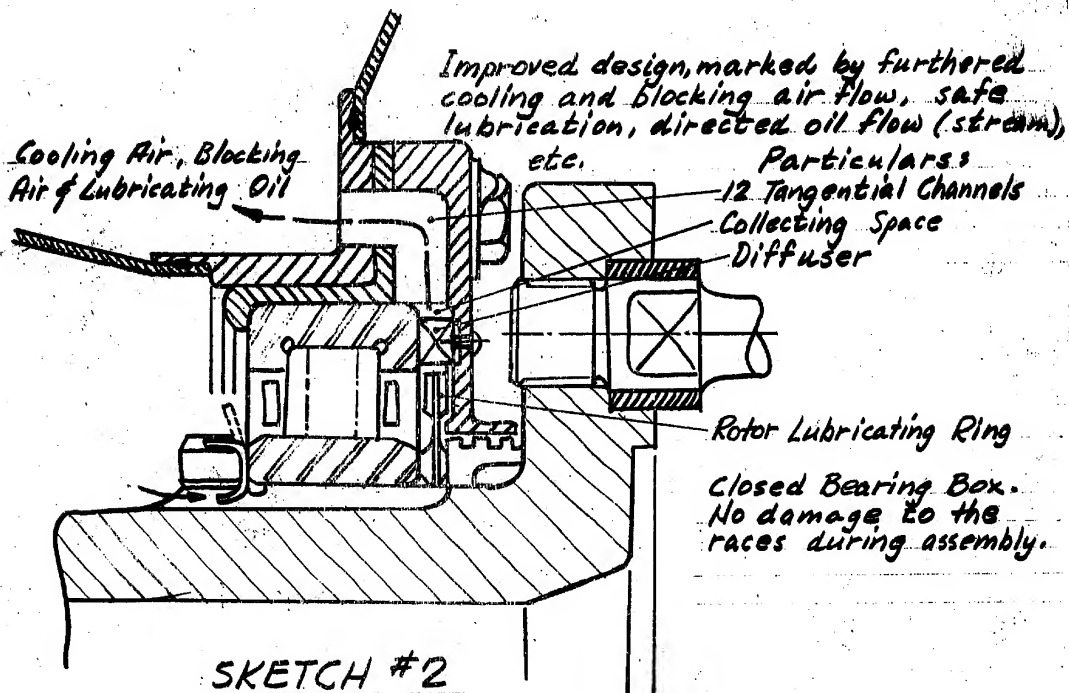
TURBINE BEARING INSTALLATIONS

Shows the Turbine Bearing as designed by the Turbine Department.



SECRET - SECURITY INFORMATION

This design was selected for the state test run. Turbine because fewer parts than in the design of Sketch #2, had to be changed.



New Designs for Turbine Bearing Installation

DIAGRAM (7)

-SECRET-

SECRET—SECURITY INFORMATION

- 30 -

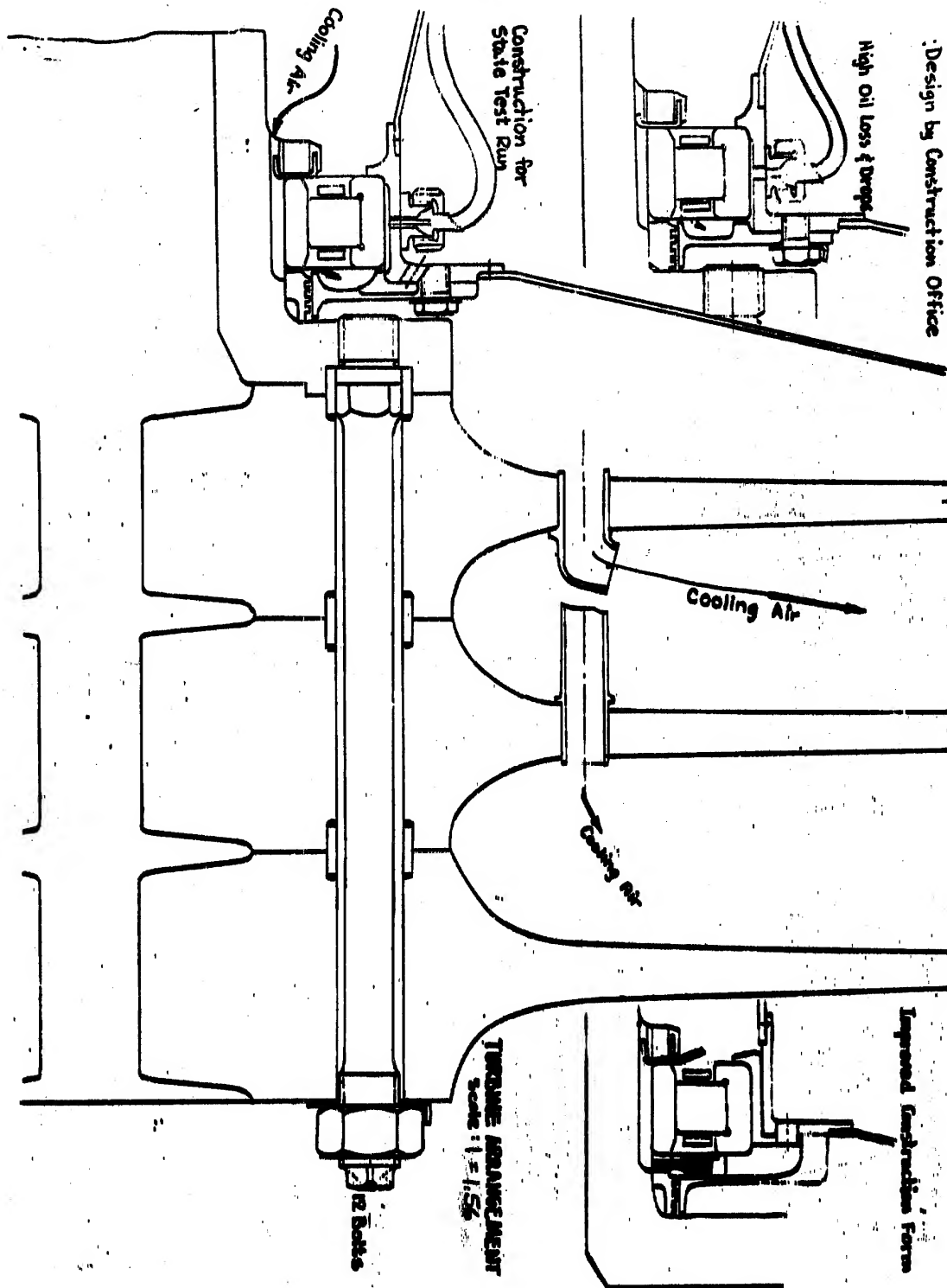
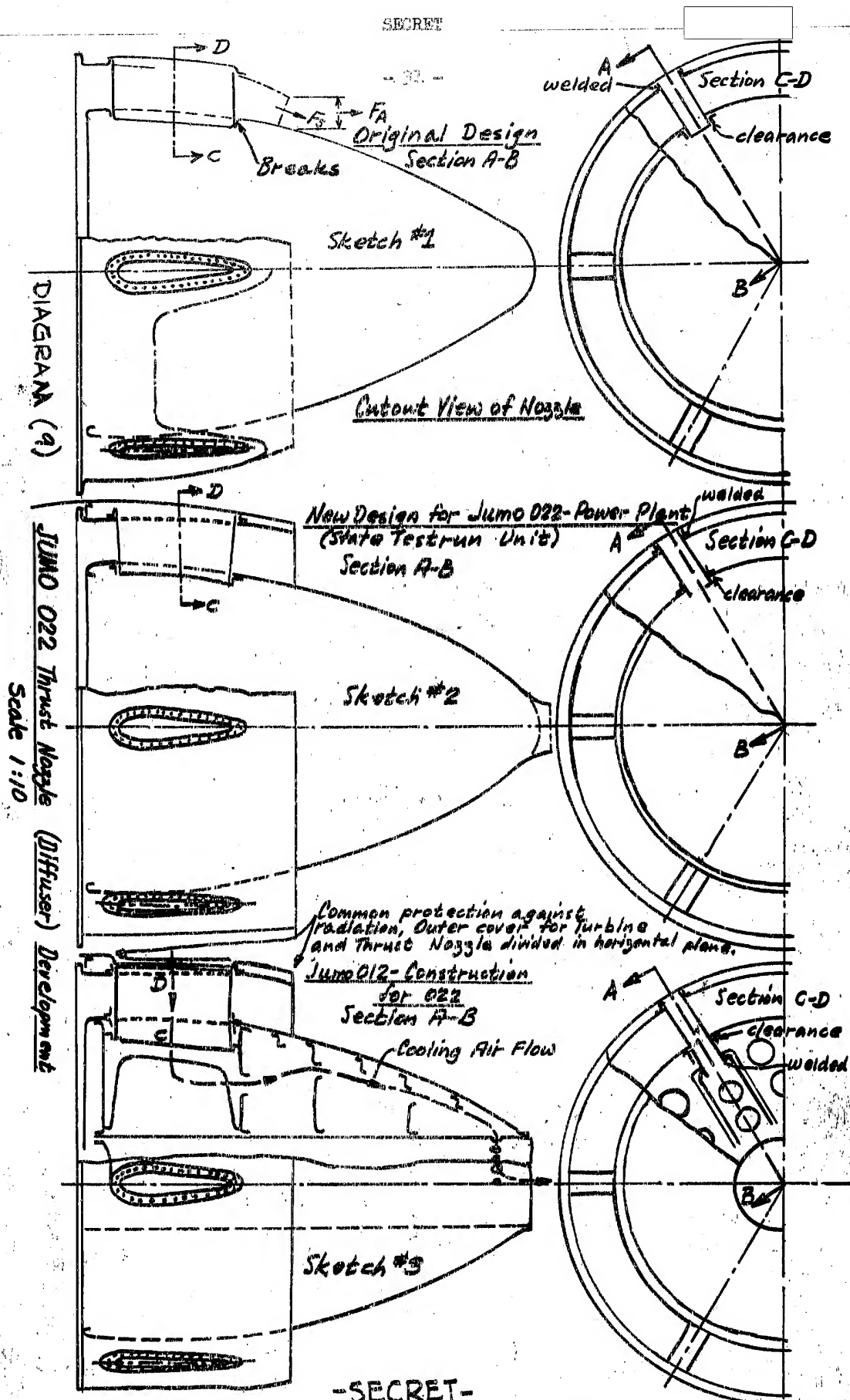
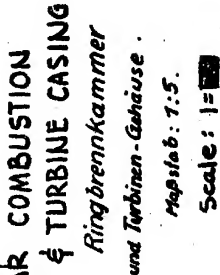


DIAGRAM (B)

SECRET—SECURITY INFORMATION

SECRET



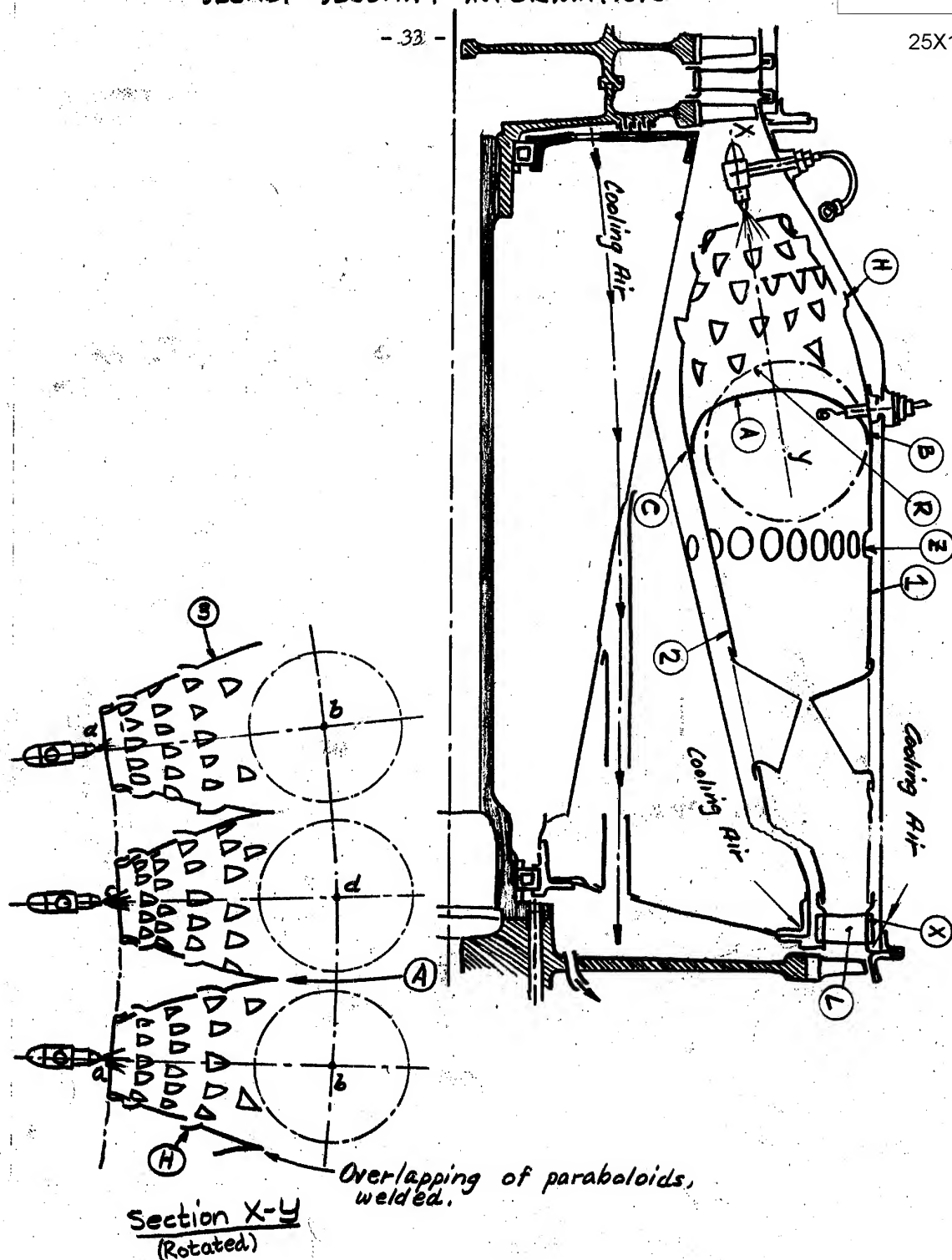


SECRET-SECURITY INFORMATION

SECRET - SECURITY INFORMATION

- 33 -

25X1

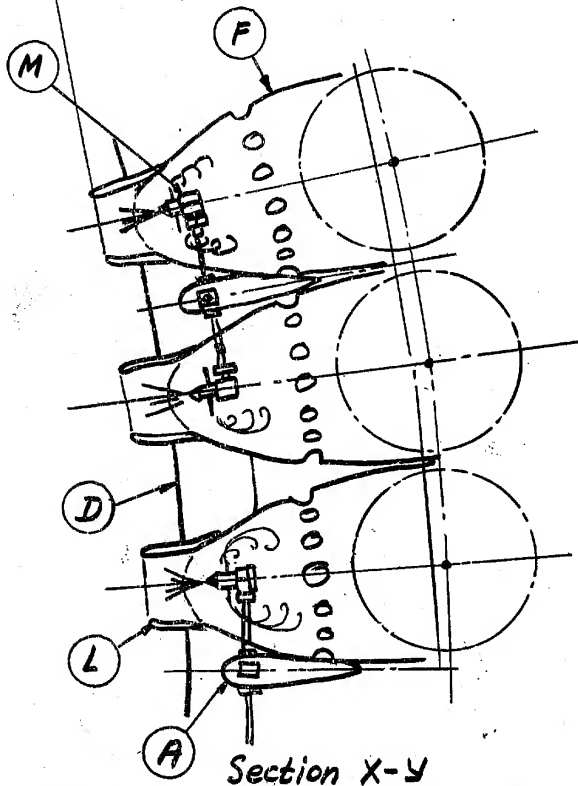
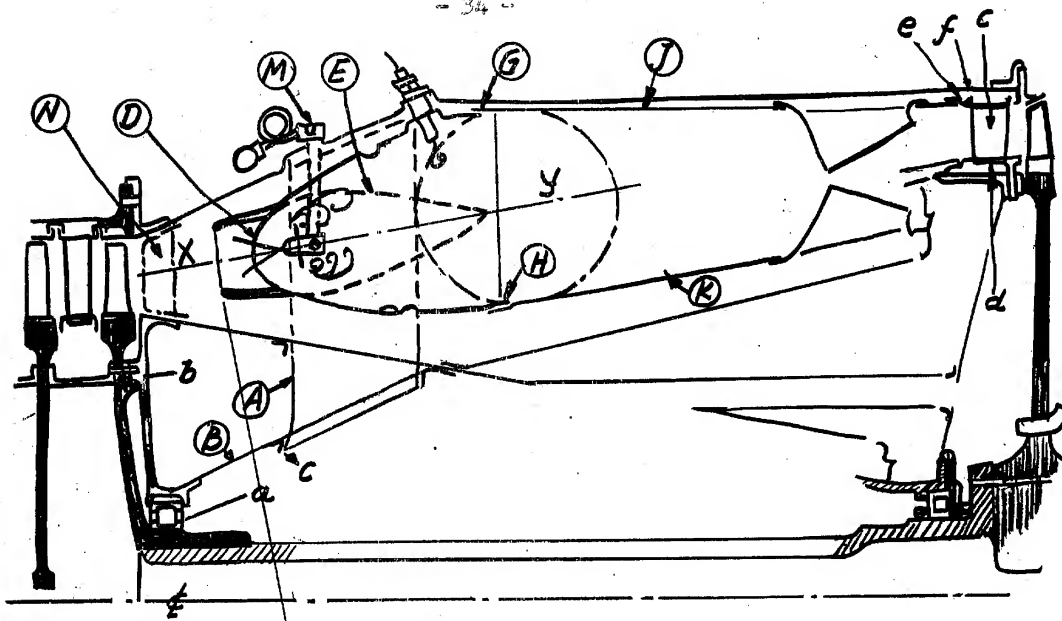


Combustion Chamber and Turbine Casing Development
(First Constructed Forms)
Scale 1:5

DIAGRAM (II)

- SECRET -

SECRET-SECURITY INFORMATION



Combustion Chamber & Turbine Casing Development
(At date still not constructed) Scale 1:5

DIAGRAM (12)

-SECRET-

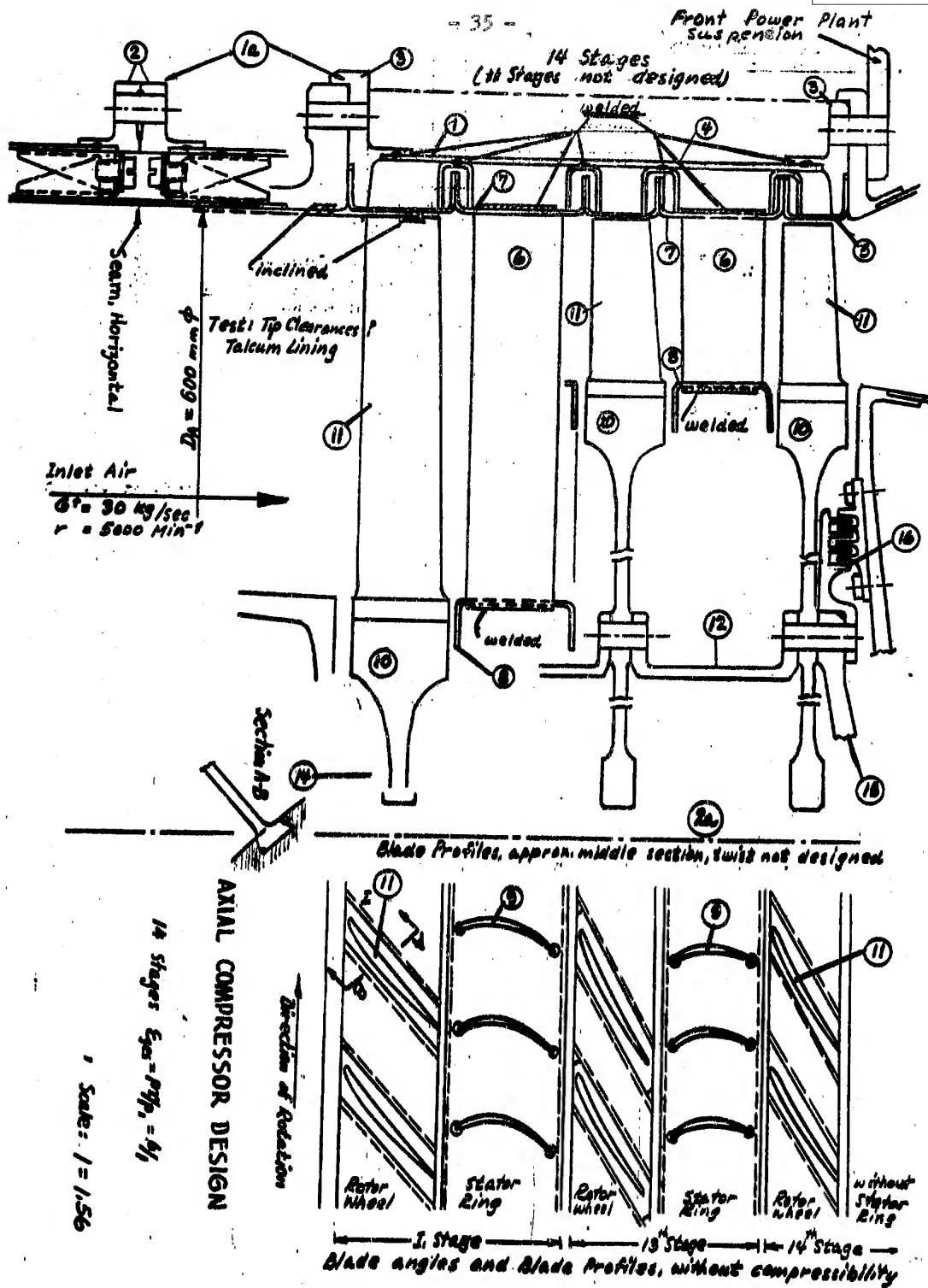
SECRET—SECURITY INFORMATION

DIAGRAM (13)

SECRET—SECURITY INFORMATION

SECRET- SECURITY INFORMATION

- 36 -

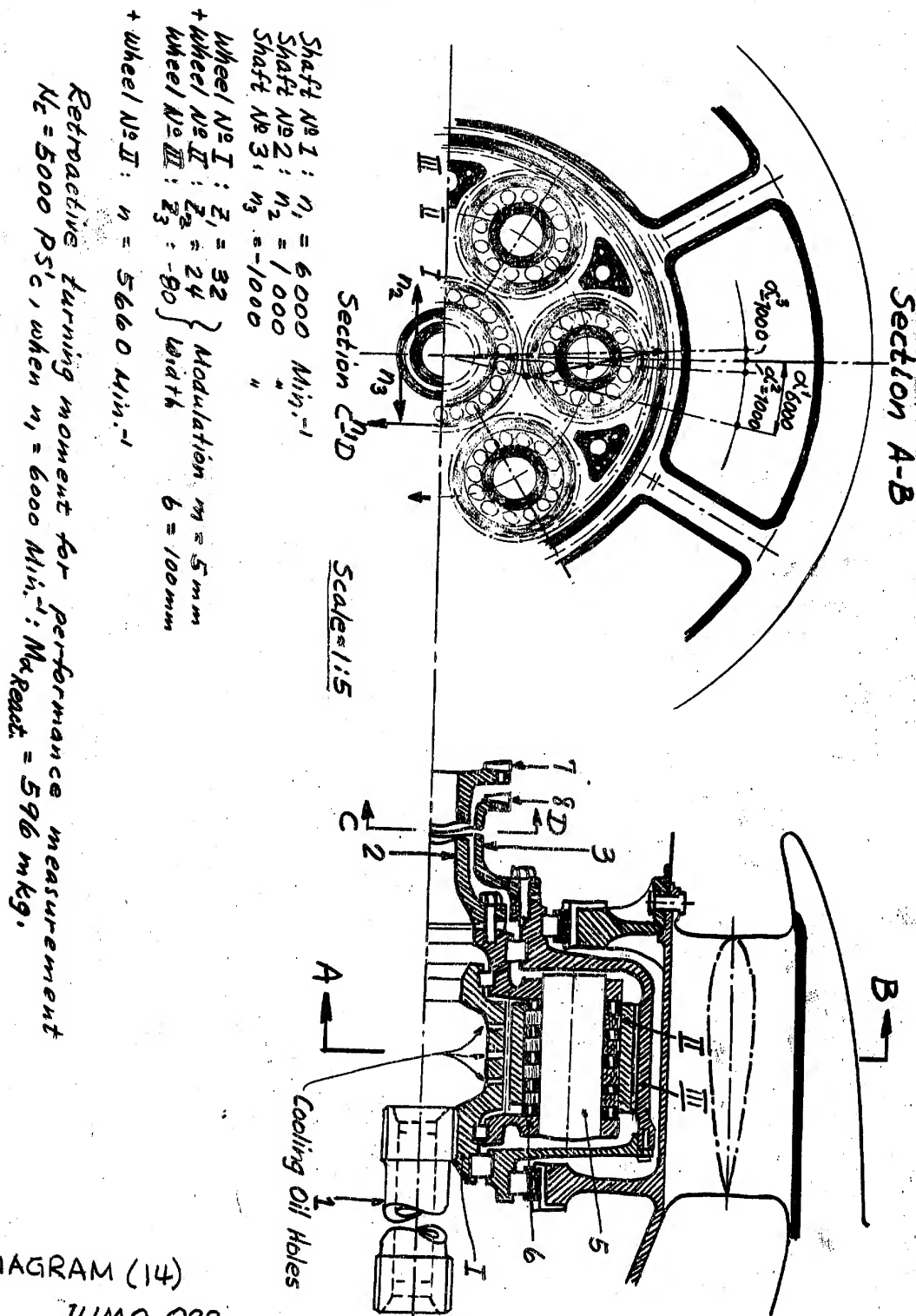


DIAGRAM (14)

JUMO 022

Counter Rotating Propeller Main Gear - with regulated

(free) numbers of revolutions $n_2 = -n_3 = 1000 \text{ Min.}^{-1}$ when $n_1 = +6000 \text{ Min.}^{-1}$

- SECRET -

SECRET-SECURITY INFORMATION

- 37 -

25X1

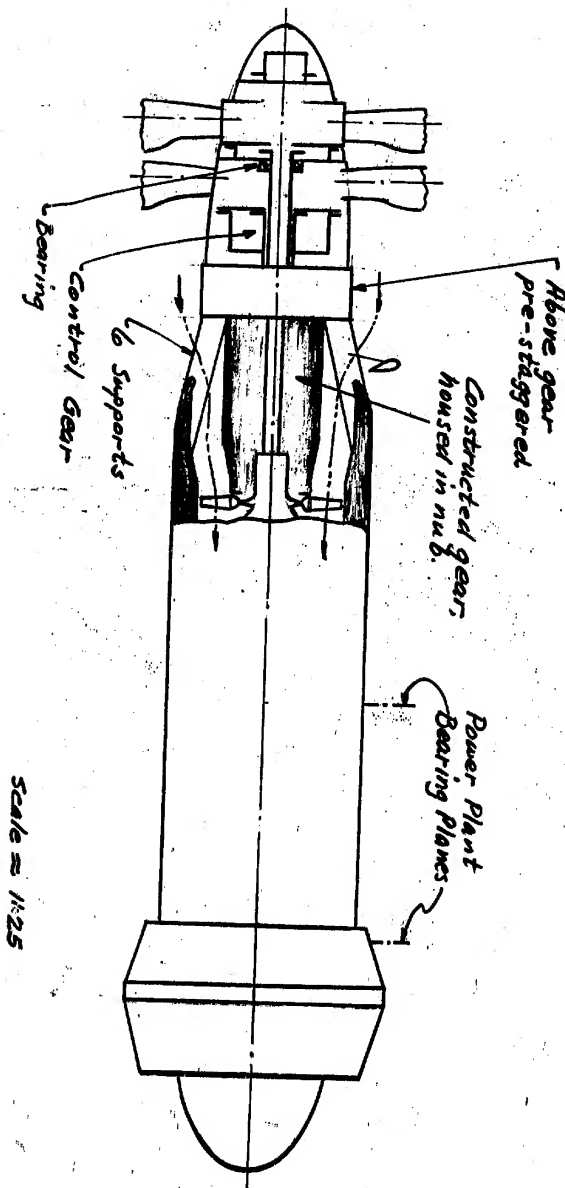


DIAGRAM (15)
PROPELLER CONTROL GEARS

-SECRET-

SECRET- SECURITY INFORMATION

25X1

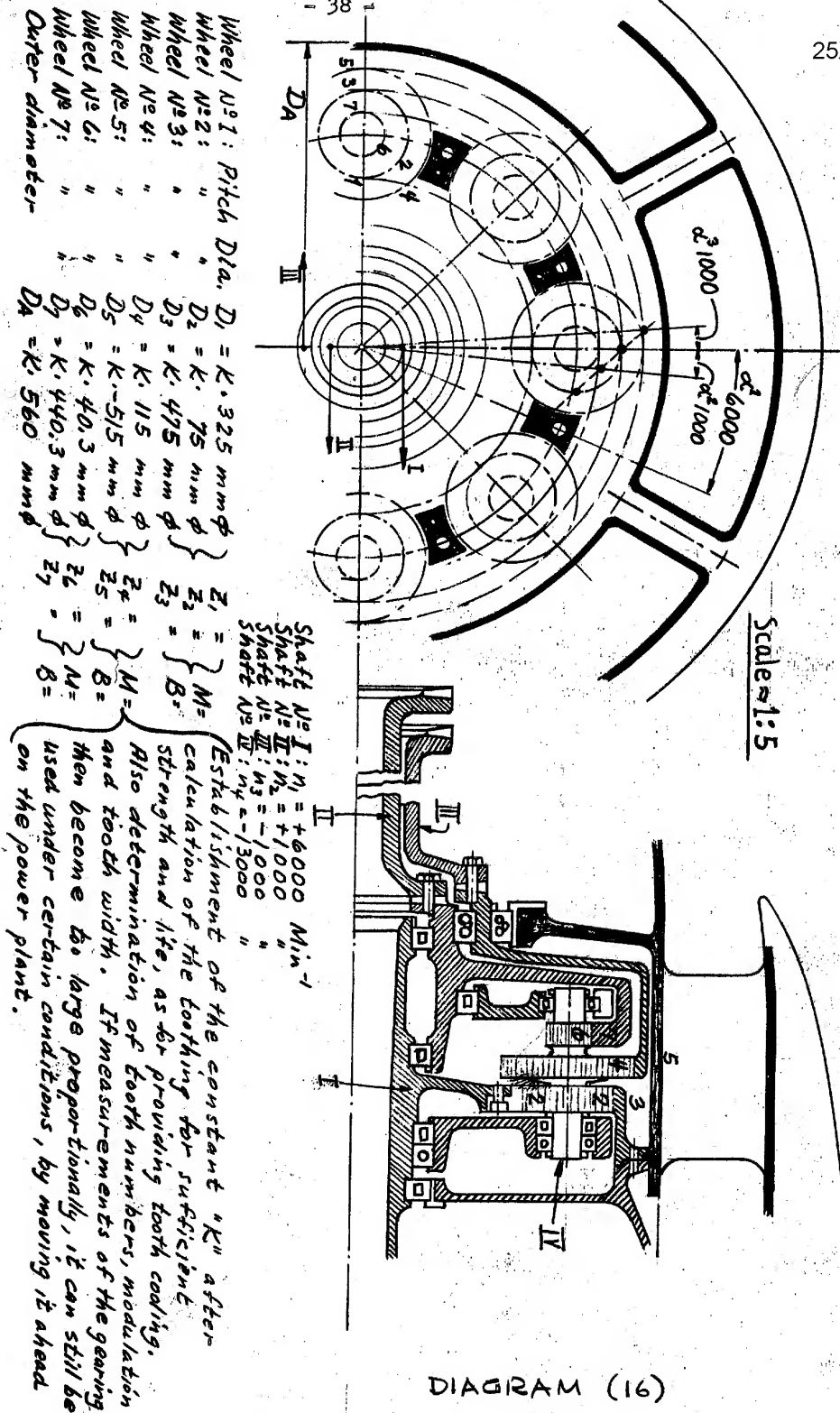


DIAGRAM (16)

PROPELLER GEARING for JUMO 012

-SECRET-